Proceedings 10th NUMGE 2023
10th European Conference on Numerical Methods in Geotechnical Engineering
Zdravković L, Konte S, Taborda DMG, Tsiampousi A (eds)
ISSN

doi: 10numge-2023-Y-XXXX

Thermo-hydro-mechanical analysis of Bentonite at residual state

S. Tourchi, M. Loche, G. Scaringi

Institute of Hydrogeology, Engineering Geology and Applied Geophysics, Faculty of Science, Charles University, Prague, Czech Republic.

ABSTRACT: This paper presents experimental and numerical investigations regarding the effect of temperature on the residual strength of Bentonite at slow-to-moderate shearing velocities. In order to understand the trigger mechanism of slow-moving landslides, we investigated the effect of temperature on the shear strength of slip surfaces. We performed ring-shear tests on Bentonite samples at various temperatures and rates. The test results show that the residual shear strength of Bentonite is both rate and temperature dependent. Under relatively slow shearing rates, strength was gained as temperature increased; in contrast, under relatively high shearing rates, strength was decreased as temperature increased. A non-isothermal viscoplastic model is proposed to simulate the observed behaviour of a ring- shear samples of Bentonite subjected to drained heating under residual conditions. The developed model was implemented in finite element computer code for THM analysis of porous media, and experimental results were numerically simulated.

Keywords: Residual strength; temperature; Bentonite; non-isothermal.

1 INTRODUCTION

A striking feature of landslides in over-consolidated clays is the localization of deformation into shear bands called a *slip surface*. Slip surface soils of reactivated landslides are typically clay-enriched and are characterized as being in residual strength conditions. The residual shear strength of slip-surface soils is essential for investigating landslide mechanisms and evaluating the reactivation potential (Mesri and Shahien 2003). Many researchers have investigated soils' residual shear strength characteristics and discovered that residual strength levels, typically discussed in terms of frictional coefficient, are influenced by several factors. Aside from test conditions, the effects of soil characteristics, such as mineral compositions, pore fluid chemistry, index properties, and grain shape, have also attracted attention and have been studied. Estimating the residual strength at slip surface is crucial from a geotechnical perspective, which is why relationships between residual friction and soil characteristics, such as clay fraction and index parameters, have been heavily investigated (Collotta et al. 1989, Wesley 2003).

The effective normal stress and shear resistance of slip surface reduce as pore water pressure rises, which promotes slope instability (Corominas et al. 2005, Matsuura et al. 2008, Schulz et al. 2009, Tommasi et al. 2006). On the other hand, it is reported that ground temperature changes are likely to affect significant portions of the slip surface, especially for shallow landslides (Lapham 1989, Matsuura et al. 2003, Shibasaki et al. 2016).

Concerning the effect of temperature on the mechanical properties of clayey soils, many studies focus on peak strength. On the contrary, the effect of temperature on the residual strength of soils remain poorly understood, although related studies were conducted by (Bucher 1975, Shibasaki et al. 2017, Shibasaki and Yamasaki 2010).

This study aims to reveal detailed temperature-dependent residual shear strength characteristics of commercial Czech B75 Bentonite. To do so, we tested Bentonite samples under temperature- and shearing rate-dependent shear ring shear tests. A non-isothermal constitutive law was then proposed based on test results analysis. The law considers the effect of temperature on the stiffness and strength parameters and the thermal softening of the slip surface. The performance of the model was checked against the recorded shear stress–relative displacements.

2 TEMPERATURE-CONTROL RING SHEAR TEST

A commercially available Czech B75 Bentonite from the Černý vrch deposit was employed for temperature-control ring shear tests. Some of the soil properties are listed in Table 1. Further characterization can be found in Roháč et al. (2019) and Sun et al. (2020).

Table 1. Some properties of Bentonite were used in the experimental study.

Parameter	Value
Specific gravity, G_s	2.7
Liquid limit, LL (%)	217
The plastic limit, PL (%)	51
Ca-Mg montmorillonite	~85
Activity, *A*	2.7
sieving-sedimentation analysis ($< 2\ \mu m$)(%)	61
sieving-sedimentation analysis ($< 60\ \mu m$)(%)	33
Unified classification system	CH

The tests were performed in a conventional ring-shear apparatus equipped with a temperature-change device allowing water circulation in a closed circuit between an external temperature-controlled bath and the shear-box bath. The device accommodates a 5 mm thick annular sample sandwiched between roughened brass porous platens to ensure drainage and avoid interface shearing. The lateral friction is minimized by ensuring post-consolidation sample thicknesses of 4mm. The available range of rotational rates was exploited, producing equivalent linear rates of 0.018-44.5 mm/min, which are associated with slow to rapid landslide movements (Cruden 1996).

We prepared the reconstituted samples following Burland (1990) and consolidated them stepwise while ensuring the dissipation of pore pressure excess by monitoring the consolidation curve. The samples were consolidated until 600 kPa and unloaded to reach the required normal stresses of 50-150 kPa. Under each stress level, the shear rate was increased stepwise, and an overconsolidated material was produced. A schematic illustration of the test specimen is shown in Figure 1.

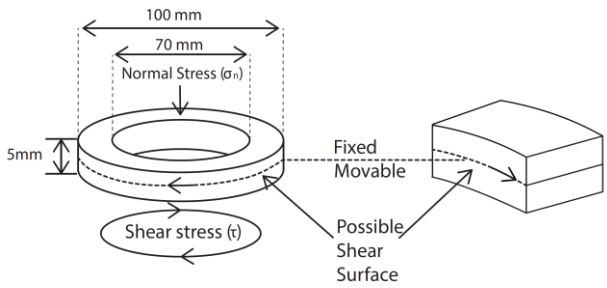

Figure 1. Schematic illustration of the test specimen subjected to thermal ring-shear experiment.

3 TEST PROCEDURE AND RESULTS

Following the method shown in Figure 2, we conducted heating-cooling tests on Bentonite samples. After attaining the residual shear strength under the chosen stress and displacement rate conditions at room temperature 20°C, the cell's temperature was increased up to 55°C and was kept constant over a sufficient shearing distance before gradually decreasing it back to the initial value. The results of the heating-cooling tests, in terms of residual friction coefficient (shear strength normalized by the normal stress), are shown in Figure 3.

Shear strength was increased with temperature increase in tests with a slow shearing rate (0.018 mm/min) (Figure 3a and 3b). However, this behaviour was not observed for the tests with moderate shearing velocities (1.78 mm/min) (Figure 3e and 3f). This time shear strength decreased with thermal loading. Interestingly weak or negligible strength change was observed for the tests with the shearing rate of 0.5 mm/min (Figure 3c and 3d), which seems to form the upper limits of the positive temperature effect at around 0.018–0.5 mm/min, almost corresponding to the "slow-moderate" landslide velocity class transition (0.3 mm/min) proposed by International Union of Geological Sciences Working Group on Landslides (1995).

As shown in Figure 3, observed shear behaviours during heating-cooling tests can be classified into three temperature effect modes: (1) positive temperature effect (shear strengthening via heating), (2) neutral temperature effect (no change via heating), and (3) negative temperature effect (shear weakening via heating). There is also a threshold shearing rate in which the transition from thermal hardening to softening behaviour has happened.

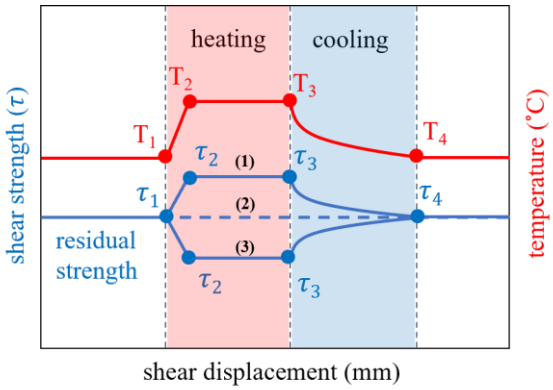

Figure 2. Schematic illustration of temperature-change (heating-cooling) experiments.

A summary of the results is shown in Figure 4. Figure 4a, 4b, and 4c show the failure envelopes of Bentonite samples obtained at 0.018 mm/min, 0.5 mm/min and 1.78mm/min, for which well-defined trends were evaluated. At the lowest rate, an increase in friction coefficient by about 13 percent is evaluated (from ~0.15 to ~0.17). At the transient rate, only a slight decrease in friction coefficient remains (-2 percent, from ~0.22 to ~0.21), whereas, at the moderate rate, 46 percent decrease in friction coefficient is evaluated (from ~0.28 to ~0.15).

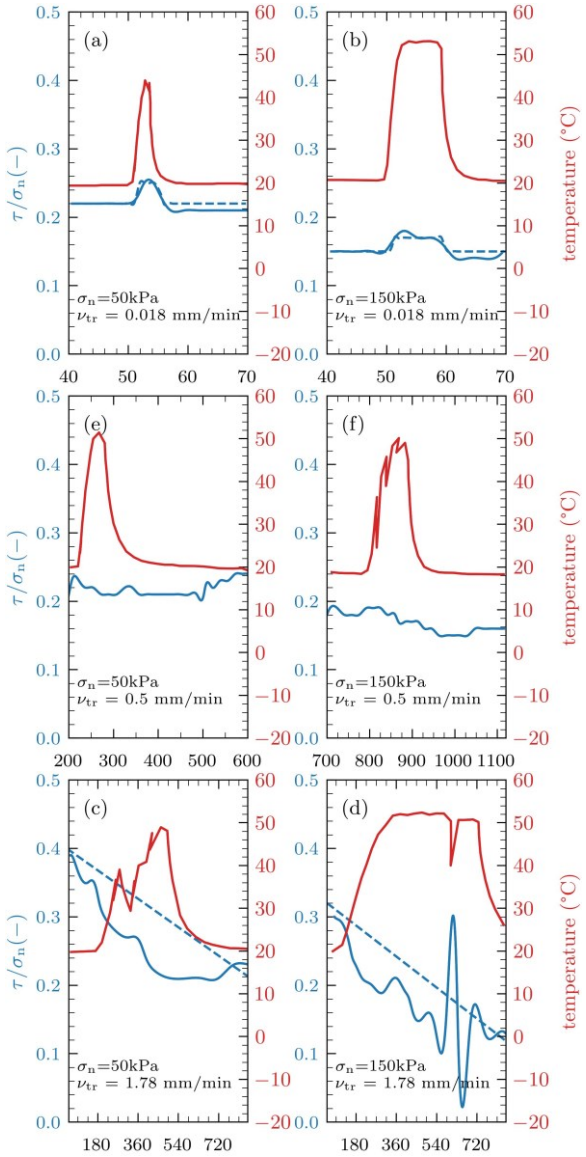

Figure 3. Results of ring shear test under heating-cooling phases at residual strength conditions.

4 THEORETICAL FORMULATION

4.1 Non-isothermal elasto- viscoplastic model for slip surface

Several thermomechanical models that can reproduce most of the observed behaviour of saturated clays at elevated temperatures have been developed by several researchers. (Hueckel and Baldi 1990) developed one of the first models by extending the well-known Cam-Clay model to consider thermo-elastoplastic behaviour. Their proposed model encompasses shrinking the elastic domain during heating (thermal softening) and expanding during cooling when the stress path is within the yield surface. In fact, adopting similar assumptions, most subsequent models are based on the same principle (Abuel-Naga et al. 2009, p. 209, Cui et al. 2000, Di Donna and Laloui 2015, Francois et al. 2009, Graham et al. 2001, Hamidi et al. 2015, 2017, Hamidi and Tourchi 2018, Modaressi and Laloui 1997, Robinet et al. 1996, Yao and Zhou 2013, Zhou and Ng 2015).

An elasto-viscoplastic formulation is proposed to model the mechanical behaviour of slip surfaces. We take as our starting point an observation of what happens when overconsolidated Bentonite samples is tested in a ring shear box, as illustrated schematically in *Figure 2*. This observation prompts us to propose a non-isothermal model of slip surface degradation in which relative shear displacements can occur in concentrated shear bands with temperature elevation.

The assumed model of a shear band in soil has much in common with cohesive force models of tensile cracks. In particular, we shall follow the development by Zandarin et al. (2013) for interface rock joint elements. In this paper we consider the shear band simply as a surface of discontinuity on which there exists a definite relation between shear stress and relative displacement.

The elastic formulation describes the normal and tangential elastic stiffnesses by means of a nonlinear law which depends on the slip surface thickness and temperature change. The viscoplastic formulation allows the treatment of non-associated plasticity and thermomechanical softening behaviour of slip surfaces subjected to shear displacements.

Total displacements ($\boldsymbol{w}$) are calculated by adding reversible elastic displacements ($\boldsymbol{w}^{\mathrm{e}}$), and viscoplastic displacements ($\boldsymbol{w}^{\mathrm{vp}}$), which are zero when stresses are below a threshold value (the yield surface):

$$\boldsymbol{w} = \boldsymbol{w}^{\mathrm{e}} + \boldsymbol{w}^{\mathrm{vp}} \tag{1}$$

A two-element vector represents normal and shear (relative) displacements in the two-dimensional case:

$$\boldsymbol{w}^{\boldsymbol{T}} = [\boldsymbol{u}_{\boldsymbol{n}}.\boldsymbol{u}_{\boldsymbol{s}}] \tag{2}$$

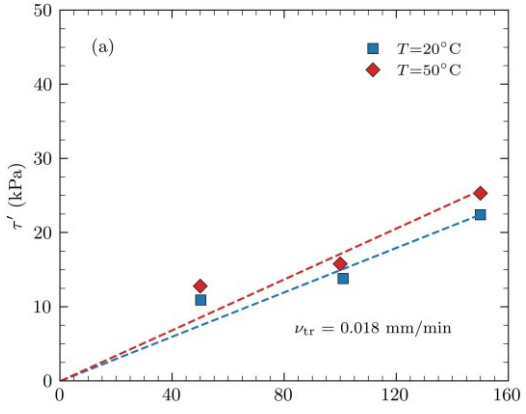

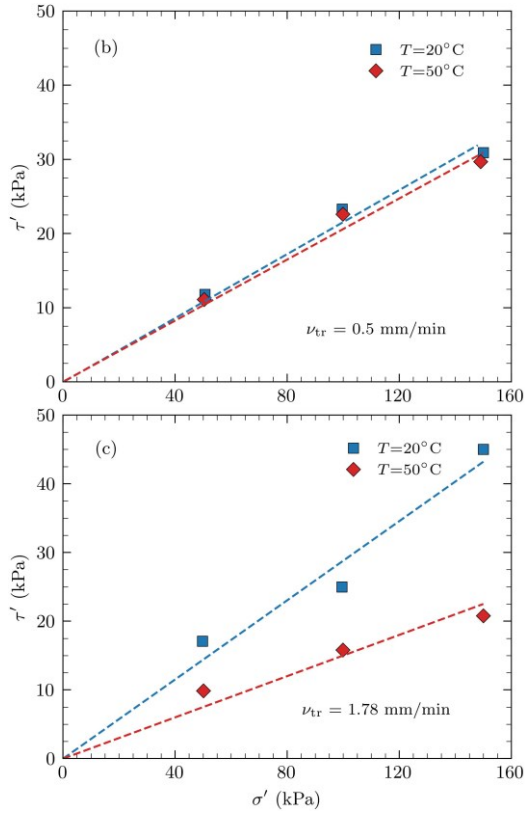

Figure 4. Residual shear strength envelope for Bentonite at 0.018 and 0.5 mm/min shear rates.

4.2 Elastic behaviour

The elastic behaviour of the slip surface relates stresses (σ' and τ) to displacements (u_n and u_s) through the normal (K_n) and tangential stiffness (K_s), respectively. Normal stiffness depends on the tickness of slip surface, as in the following equations:

$$\begin{Bmatrix} u_n \\ u_s \end{Bmatrix} = \begin{bmatrix} 1/K_n & 0 \\ 0 & 1/K_s \end{bmatrix} \begin{Bmatrix} \sigma' \\ \tau \end{Bmatrix} \tag{3}$$

$$K_n = \frac{m}{t - t_{min}} \tag{4}$$

where m is a parameter of the model; t is the thikness of the slip surface and t_{min} is the minimum slip surface tickness.

4.3 Viscoplastic behaviour

Viscoplastic formulation consist of yield surface, a plastic potential, and a softening law. Viscoplastic displacements occur when the stress state of the interface elements reaches a yielding condition. In this study, a hyperbolic yield surface based on Gens et al. (1990) was adopted:

$$F = \tau^2 - (c' - \sigma' \tan \phi')^2 + (c' - \chi \tan \phi')^2 \tag{5}$$

where τ is the shear stress; c' is the effective cohesion; σ' is the net normal stress and $\tan\phi'$ is the tangent of effective angle of internal friction and χ is a model parameter.

4.4 Softening law

The strain softening of slip surface subjected to shear stress is modelled by means of the degradation of the strength parameters. The degradation of parameters depends linearly on viscoplastic relative shear displacements. The cohesion decays from the initial value to zero and the friction angle decays from the peak to the residual value as a function of a critical viscoplastic shear displacement. Two different values of u^* are used to define the decrease of cohesion (u_c^*) and friction angle (u^*). The mathematical expression is

$$c' = c_0' \left(1 - \frac{u_s^{vp}}{u_c^*}\right) \tag{6}$$

where c' is the effective cohesion which corresponds to the viscoplastic shear displacement u_s^{vp}. c_0' is the initial value of effective cohesion, and u_c^* is the critical value of shear displacement, for which the value of c' is zero. Also,

$$\tan \varphi' = \tan \varphi_0' - (\tan \varphi_0' - \tan \varphi_{res}') \frac{u_s^{vp}}{u_\varphi^*} \tag{7}$$

where $\tan \varphi'$ corresponds to viscoplastic shear displacement u_s^{vp}, $\tan \varphi_0'$ is the tangent of the peak friction angle, $\tan \varphi_{res}'$ is the tangent of the internal friction effective residual angle, and u_φ^* is the critical value of shear displacement when the value of $\tan \varphi'$ is equal to $\tan \varphi_{res}'$.

4.4.1 Viscoplastic displacements

If $F < 0$, the stress state of the interface element is inside the elastic region; if $F \geq 0$, the displacements

$$\frac{d\boldsymbol{w}^{vp}}{dt} = \Gamma < \phi\left(\frac{F}{F_0}\right) > \frac{\partial G}{\partial \sigma} \tag{8}$$

where G is a plastic potential, and Γ is a viscosity parameter. The normal and shear viscoplastic displacement rates, $\boldsymbol{u}_n^{vp}$ and $\boldsymbol{u}_s^{vp}$, are given by a power laws:

$$\Delta \dot{\boldsymbol{u}}_n^{vp} = \Gamma F^N \frac{\partial G}{\partial \sigma} \tag{9}$$

$$\Delta \dot{\boldsymbol{u}}_s^{vp} = \Gamma F^N \frac{\partial G}{\partial \tau} \tag{10}$$

where N is the exponent of the power law.

4.5 Plastic potential and dilatancy

The associated rule allows the calculation of displacements directions. The derivative of G with respect to stresses includes the parameters f_σ^{dil} and f_c^{dil},

which take into account the dilatant behaviour of the slip surface under shear stresses (Garello 1999):

$$\frac{\partial G}{\partial \boldsymbol{\sigma}} = \left[2\tan\,\phi'(c' - \sigma'\tan\,\phi')f_{\sigma}^{dil} f_{c}^{dil}.2\tau\right]^{T} \quad (11)$$

where $f_{\sigma}^{\mathrm{dil}}$ accounts for the decrease of dilatancy with the level of the normal stress acting on the interface, and f_{c}^{dil} defines the degradation of the interface surfaces due to shear displacements. The following expressions describe these effects:

$$f_{\sigma}^{\mathrm{dil}} = \left(1 - \frac{|\sigma'|}{q_{\mathrm{u}}}\right)\exp\left(-\beta_{\mathrm{d}}\frac{|\sigma'|}{q_{\mathrm{u}}}\right) \quad (12)$$

$$f_{c}^{\mathrm{dil}} = \frac{c'}{c'_{0}} \quad (13)$$

where q_{u} is the compression strength of the material for which dilatancy vanishes, β_{d} is a model parameter, and c' is the cohesion value for the viscoplastic shear displacement $u_{\mathrm{s}}^{\mathrm{vp}}$.

4.6 Non-isothermal formulation

4.6.1 Thermoelastic components

Preliminary data suggest that the elastic domain varies with temperature. So, the normal and tangential stiffness are assumed to be a function not only of viscoplastic shear displacements but also of temperature,

$$K_{n}(T) = \begin{cases} K_{n}(T_{0})\left[1 + \mu_{K}\ln\left(T/T_{0}\right)\right] & \nu < \upsilon_{tr} \\ K_{n}^{T_{0}} & \nu = \upsilon_{tr} \\ K_{n}(T_{0})\left[1 - \mu_{K}\ln\left(T/T_{0}\right)\right] & \nu > \upsilon_{tr} \end{cases} \quad (14)$$

where $K_n(T_0)$ and $K_n(T)$ are normal stiffness at reference and a given temperature, respectively, μ_K controls the rate of variation of normal stiffness with temperature ,and υ *and* υ_{tr} are shear rate and threshold shearing rate, respectivly. Tangential stiffness varies with temperature with a similar logarithmic relationship to Equation (11):

$$K_{s}(T) = \begin{cases} K_{s}(T_{0})\left[1 + \mu_{S}\ln\left(T/T_{0}\right)\right] & \nu < \upsilon_{tr} \\ K_{s}(T_{0}) & \nu = \upsilon_{tr} \\ K_{s}(T_{0})\left[1 - \mu_{S}\ln\left(T/T_{0}\right)\right] & \nu > \upsilon_{tr} \end{cases} \quad (15)$$

where $K_s(T_0)$ and $K_s(T)$ are tangential stiffness at reference and a given temperature, respectively and μ_S controls the rate of variation of normal stiffness with temperature.

4.6.2 Thermoplastic components

In the context of landslides, key thermal effects in clays are those are those that lead to irreversible plastic deformations and, therefore, those affecting the failure of slip surfaces. As discussed in Section 3, the residual shear strength of Bentonite varies with temperature change. This implies that larger plastic deformations and a failure surface can be expected under higher temperatures, such as those induced by near-surface ground temperature changes. Following (Tourchi 2020, Tourchi et al. 2020, 2022), this behaviour can be incorporated by assuming that the strength parameters also depend on temperature. A hyperbolic Mohr-Coulomb type yield function mainly is characterizes the adopted model; therefore, the strength's dependence on temperature can also be incorporated through the parameters ϕ and c. On the othe hand, since no cohesion was observed in the experiment which is comprehensible because small or negligible cohesions have been reported in many literature reports regarding residual strength parameters, only mobilized friction angle must be a function of temperature. In the case of the friction angle, Equation (16) can be adopted to define ϕ_{res} as a function of temperature in the following way:

$$\varphi_{res}^{T} = \begin{cases} \varphi_{res}^{T_{0}}\left[1 + \mu_{\varphi}\ln\left(T/T_{0}\right)\right] & \nu < \upsilon_{TR} \\ \varphi_{res}^{T_{0}} & \nu = \upsilon_{TR} \\ \varphi_{res}^{T_{0}}\left[1 - \mu_{\varphi}\ln\left(T/T_{0}\right)\right] & \nu > \upsilon_{TR} \end{cases} \quad (16)$$

where $\varphi_{res}^{T_0}$ and φ_{res}^{T} are the residual friction angle at the reference temperature (T_0) and elevated temperature (T), and coefficients μ_φ is a model parameter that controls the thermal evolution of the friction angle.

The incorporated dependence of the yield function with temperature requires the modification of the standard form of Prager's consistency condition. In the case of plastic loading, the latter reads:

$$df = \frac{\partial f}{\partial \boldsymbol{\sigma}}d\boldsymbol{\sigma} + \frac{\partial f}{\partial \phi_{\mathrm{mob}}}d\phi_{\mathrm{mob}} = 0 \quad (17)$$

where

$$\mathrm{d}\varphi = \frac{\partial \varphi}{\partial u_{s}^{vp}}\mathrm{d}u_{s}^{vp} + \frac{\partial \varphi}{\partial \mathrm{T}}\mathrm{dT} \quad (18)$$

Therefore, plastic deformations are also affected by the thermal variation of the strength parameters.

5 NUMERICAL SIMULATION OF RING SHEAR TEST

The ring shear tests with rates 0.018 mm/min and 1.78 mm/min selected to check the capabilities of the model were performed on Bentonite samples. The numerical simulation was carried out with finite element code Code_Bright (Olivella et al. 1996) employing the interface element (Carol et al. 1997) and the new non-isothermal constitutive law proposed above.

Table 2. Parameters for ring shear samples (elasto visco-plastic model).

Parameter	Value	Unit
Mechanical properties		
Initial normal stiffness parameter, m	60×10^3	kPa
Tangential stiffness, K_s	166×10^3	kPa/m
Initial friction angle, $\boldsymbol{\varphi_0}$	35	(°)
	8.69	(°)
Residual friction angle, $\boldsymbol{\varphi_{res}^{T0}}$	12.18	(°)
	16	
Initial shear surface thickness, t_0	0.1	mm
Minimum shear surface thickness, t_{min}	0.01	mm
Viscosity, $\boldsymbol{\Gamma}$	1×10^{-2}	s^{-1}
Stress power, N	2.0	-
Uniaxial compressive strength, q_u	600	kPa
Model parameter, $\boldsymbol{\beta_d}$	100	-
Non-isothermal parameters		
	9.85	(°)
Residual friction angle, $\boldsymbol{\varphi_{res}^{T}}$	11.69	(°)
	8.53	(°)
Model parameter, $\boldsymbol{\mu_\varphi}$	0.5	-

The simulation is assumed under axisymmetric two-dimensional coupled THM conditions. The Fixed and Movble parts (*Figure 1*) are simulated as an elastic material, and the sample is modelled as a visco-plastic zero-thickness element. The parameters are listed in Table 2. The predictions of the numerical analysis are plotted in a dashed line alongside test measurements in Figure 3. In general, the numerical results predict well the experimental results.

6 ACKNOWLEDGEMENTS

Research leading to these results has received funding from the European Commission via a Marie Curie Fellowship awarded to Dr. Saeed Tourchi.

7 CONCLUSIONS

The influence of temperature and shearing rate on the residual shear strength of Bentonite behaviour was experimentally investigated. It is believed that this is an important issue in landslides. An available direct shear device was successfully modified to test Bentonite samples under the controlled temperature of the specimens. The ring shear test results showed a marked dependency of residual shear stress with temperature and shear rate. New mathematical expressions for the strength parameters and normal and tangential stiffnesses of the asymptote of the hyperbolic yield surface adopted are proposed. The model was introduced as a constitutive law of the interface element implemented in the computer code Code_Bright. The experimental features of the tested Bentonite samples are satisfactorily explained by the numerical simulation.

8 REFERENCES

Abuel-Naga HM, Bergado DT, Bouazza A, Pender M (2009) Thermomechanical model for saturated clays. *Geotechnique* 59(3):273–278.

Bucher F (1975) *Die Restscherfestigkeit natürlicher Böden, ihre Einflussgrössen und Beziehungen als Ergebnis experimenteller Untersuchungen*. PhD Thesis. (ETH Zurich).

Burland JB (1990) On the compressibility and shear strength of natural clays. *Géotechnique* 40(3):329–378.

Carol I, Prat PC, López CM (1997) Normal/Shear Cracking Model: Application to Discrete Crack Analysis. *J. Eng. Mech.* 123(8):765–773.

Collotta T, Cantoni R, Pavesi U, Ruberl E, Moretti PC (1989) A correlation between residual friction angle, gradation and the index properties of cohesive soils. *Géotechnique* 39(2):343–346.

Corominas J, Moya J, Ledesma A, Lloret A, Gili JA (2005) Prediction of ground displacements and velocities from groundwater level changes at the Vallcebre landslide (Eastern Pyrenees, Spain). *Landslides* 2(2):83–96.

Cruden D (1996) Cruden,D.M.,Varnes, D.J.,1996, Landslide Types and Processes, Transportation Research Board, U.S. National Academy of Sciences, Special Report, 247: 36-75. *Spec. Rep. - Natl. Res. Counc. Transp. Res. Board* 247:36–57.

Cui YJ, Sultan N, Delage P (2000) A thermomechanical model for saturated clays. *Can. Geotech. J.* 37(3):607–620.

Di Donna A, Laloui L (2015) Response of soil subjected to thermal cyclic loading: Experimental and constitutive study. *Eng. Geol.* 190:65–76.

Francois B, Laloui L, Laurent C (2009) Thermo-hydro-mechanical simulation of ATLAS in situ large scale test in Boom Clay. *Comput. Geotech.* 36(4):626–640.

Garello CML (1999) *Análisis microestructural de la fractura del hormigón utilizando elementos finitos tipo junta. Aplicación a diferentes hormigones*. PhD Thesis. (Universitat Politècnica de Catalunya (UPC)).

Graham J, Tanaka N, Crilly T, Alfaro M (2001) Modified Cam-Clay modelling of temperature effects in clays. *Can. Geotech. J.* 38(3):608–621.

Hamidi A, Tourchi S (2018) A thermomechanical constitutive model for unsaturated clays. *Int. J. Geotech. Eng.* 12(2):185–199.

Hamidi A, Tourchi S, Kardooni F (2017) A critical state based thermo-elasto-plastic constitutive model for structured clays. *J. Rock Mech. Geotech. Eng.* 9(6):1094–1103.

Hamidi A, Tourchi S, Khazaei C (2015) Thermomechanical Constitutive Model for Saturated Clays Based on Critical State Theory. *Int. J. Geomech.* 15(1):04014038.

Hueckel T, Baldi G (1990) Thermoplasticity of Saturated Clays - Experimental Constitutive Study. *J. Geotech. Eng.-Asce* 116(12):1778–1796.

International Union of Geological Sciences Working Group on Landslides (1995) A suggested method for describing the rate of movement of a landslide. *Bull.*

Int. Assoc. Eng. Geol. - Bull. Assoc. Int. Géologie Ing. 52(1):75–78.

Lapham WW (1989) *Use of temperature profiles beneath streams to determine rates of vertical ground-water flow and vertical hydraulic conductivity* (Dept. of the Interior, US Geological Survey; USGPO; Books and Open-File …).

Matsuura S, Asano S, Okamoto T (2008) Relationship between rain and/or meltwater, pore-water pressure and displacement of a reactivated landslide. *Eng. Geol.* 101(1–2):49–59.

Matsuura S, Asano S, Okamoto T, Takeuchi Y (2003) Characteristics of the displacement of a landslide with shallow sliding surface in a heavy snow district of Japan. *Eng. Geol.* 69(1–2):15–35.

Mesri G, Shahien M (2003) Residual shear strength mobilized in first-time slope failures. *J. Geotech. Geoenvironmental Eng.* 129(1):12–31.

Modaressi H, Laloui L (1997) A thermo-viscoplastic constitutive model for clays. *Int. J. Numer. Anal. Methods Geomech.* 21(5):313–335.

Olivella S, Gens A, Carrera J, Alonso EE (1996) Numerical formulation for a simulator (CODE_BRIGHT) for the coupled analysis of saline media. *Eng. Comput.* 13(7):87–112.

Robinet JC, Rahbaoui A, Plas F, Lebon P (1996) A constitutive thermomechanical model for saturated clays. *Eng. Geol.* 41(1–4):145–169.

Roháč J, Scaringi G, Boháč J, Kycl P, Najser J (2019) Revisiting strength concepts and correlations with soil index properties: insights from the Dobkovičky landslide in Czech Republic. *Landslides* 17.

Schulz WH, Kean JW, Wang G (2009) Landslide movement in southwest Colorado triggered by atmospheric tides. *Nat. Geosci.* 2(12):863–866.

Shibasaki T, Matsuura S, Hasegawa Y (2017) Temperature-dependent residual shear strength characteristics of smectite-bearing landslide soils. *J. Geophys. Res. Solid Earth* 122(2):1449–1469.

Shibasaki T, Matsuura S, Okamoto T (2016) Experimental evidence for shallow, slow-moving landslides activated by a decrease in ground temperature. *Geophys. Res. Lett.* 43(13):6975–6984.

Shibasaki T, Yamasaki T (2010) Experimental investigation on temperature effect on residual strength characteristics of soils. *J. Jpn. Landslide Soc.* 47(5):255–264.

Sun H, Mašín D, Najser J, Scaringi G (2020) Water retention of a bentonite for deep geological radioactive waste repositories: High-temperature experiments and thermodynamic modeling. *Eng. Geol.* 269:105549.

Tommasi P, Pellegrini P, Boldini D, Ribacchi R (2006) Influence of rainfall regime on hydraulic conditions and movement rates in the overconsolidated clayey slope of the Orvieto hill (central Italy). *Can. Geotech. J.* 43(1):70–86.

Tourchi S (2020) THM analysis of argillaceous rocks with application to nuclear waste underground storage.

Tourchi S, Gens A, Vaunat J, Mánica M, Scaringi G (2020) A thermomechanical model for argillaceous rocks McCartney JS, Tomac I, eds. *E3S Web Conf.* 205:13014.

Tourchi S, Malcom MAM, Vaunat J, Gens A (2022) A thermomechanical model for argillaceous hard soils - weak rocks: application to THM simulation of deep excavations in claystone. *EarthArXiv*.

Wesley LD (2003) Residual strength of clays and correlations using Atterberg limits. *Geotechnique* 53(7):669–672.

Yao Y p., Zhou A n. (2013) Non-isothermal unified hardening model: a thermo-elasto-plastic model for clays. *Géotechnique* 63(15):1328–1345.

Zandarin MT, Alonso E, Olivella S (2013) A constitutive law for rock joints considering the effects of suction and roughness on strength parameters. *Int. J. Rock Mech. Min. Sci.* 60:333–344.

Zhou C, Ng CWW (2015) A thermomechanical model for saturated soil at small and large strains. *Can. Geotech. J.* 52(8):1101–1110.